# Transcriptional signature of flavopiridol-induced tumor cell death

**Xing Lü,[1] William E. Burgan,[1] Michael A. Cerra,[1] Eric Y. Chuang,[2] Mong-Hsun Tsai,[3] Philip J. Tofilon,[1] and Kevin Camphausen[2]**

**[1] Molecular Radiation Therapeutics Branch, [2] Radiation Oncology Branch, and [3] Radiation Biology Branch, National Cancer Institute, Bethesda, Maryland**

## Abstract

**Flavopiridol has been shown to inhibit the proliferation of a variety of human tumor cells and is currently undergoing clinical evaluation in cancer treatment. Although the antiproliferative effect of flavopiridol has been attributed to the inhibition of cyclin-dependent kinases 2 and 4, recent reports indicate that the mechanism responsible for the cell death induced by this agent is more complex. To provide insight into the molecular processes mediating flavopiridol-induced cytotoxicity and to investigate the availability of markers indicative of its activity, we have applied cDNA microarray technology. Gene expression profiles were determined for four human tumor cell lines (prostate carcinomas PC3 and DU145 and gliomas SF539 and U251) following exposure to selected concentrations of flavopiridol. Treatment of these cell lines with a concentration of flavopiridol sufficient to reduce survival to 10% resulted in the identification of a set of 209 genes, the expression of which were altered in each of the cell lines. This common set of 209 gene expression changes suggested that flavopiridol-induced cell death can be defined in terms of a specific transcriptome. The flavopiridol death transcriptome consisted primarily of down-regulated genes; however, there were also a significant number of genes with increased expression. Whereas causal relationships were not established, these data suggest molecular events/processes that may be associated with flavopiridol-induced tumor cell death. Moreover, the identification of a set of gene expression changes in four human tumor cell lines suggests that such a transcriptome may be applicable to investigations of flavopiridol pharmacodynamics. [Mol Cancer Ther 2004; 3(7):861–72]**

Received 2/19/04; revised 4/9/04; accepted 4/15/04.

The costs of publication of this article were defrayed in part by the payment of page charges. This article must therefore be hereby marked advertisement in accordance with 18 U.S.C. Section 1734 solely to indicate this fact.

**Requests for reprints:** Kevin Camphausen, Radiation Oncology Branch, National Cancer Institute, 10 Center Drive, Building 10, Room B3B69, Bethesda, MD 20892-1002. Phone: 301-496-5457; Fax: 301-480-5439. E-mail: camphauk@mail.nih.gov



## Introduction

Flavopiridol is a semisynthetic flavonoid that has potent inhibitory activity against a variety of cyclin-dependent kinases (cdks; ref. 1). In preclinical studies, flavopiridol was shown to inhibit the proliferation of a broad range of human tumor cells *in vitro* and *in vivo*, which led to its current evaluation in phase I and II clinical trials (2). Phase I studies have demonstrated safety for 72- and 1-hour infusions with some efficacy noted in patients with renal, prostate, and colon cancer as well as non-Hodgkin's lymphoma (2-4). Currently, there are 15 clinical trials in various stages of accrual aimed at evaluating the antitumor efficacy of flavopiridol (http://www.cancer.org).

Although an inhibitor of cdks in general, flavopiridol is most effective against cdks 1, 2, and 4, consistent with its antiproliferative actions (5, 6). However, accumulating evidence suggests that the mechanism of action of flavopiridol is more complex and diverse than initially thought. The ability of flavopiridol to induce cytotoxicity in nondividing cells suggests that, in addition to the inhibition of cdks 1, 2, and 4, other critical cellular survival processes are affected. Flavopiridol has been reported to inhibit P-TEFb activity, presumably via an inhibition of cdk 9 (7). Inhibition of P-TEFb results in the reduced transcriptional elongation of mRNA species with short half-lives, which includes inducible transcripts (8). This reduction in P-TEFb appears to play a role in the frequently reported flavopiridol-mediated decrease in cyclin D1 (9) and in the expression of several antiapoptotic proteins (7). Finally, flavopiridol has also been reported to bind directly to DNA, although the biological significance has not been determined (10). Thus, although initially proposed to target tumor cell proliferation via cdk inhibition, flavopiridol clearly has additional molecular and cellular actions. Moreover, its cytotoxic effects against solid tumors, which are composed of heterogeneous cell populations, may involve the targeting of multiple cellular processes. Defining the critical processes and molecules mediating flavopiridol-induced tumor cell death should aid in its clinical application in cancer treatment not only as a single agent but also in combined modalities.

Global gene expression profiling based on microarray analysis is becoming an accessible strategy for generating novel information relevant to cancer diagnosis and treatment. For the most part, gene expression studies have focused on tumor classification and prediction of sensitivity (11, 12). However, microarray analysis can also be used to define the molecular consequences of exposure to chemotherapeutic agents. Along these lines, several recent studies have investigated the use of gene expression profiling performed on treated cells or tissues to generate mechanistic insight into drug action and to identify markers of drug activity (13-16). In an attempt to generate

similar information for flavopiridol and given that it apparently operates through multiple and/or unknown mechanisms to induce tumor cell death, we have defined the changes in global gene expression induced by this chemotherapeutic agent in four human tumor cell lines. Importantly, these studies were performed using flavopiridol concentrations that resulted in >90% tumor cell death. At these lethal concentrations, we identified a transcriptome profile of 209 genes that were altered in each of the four cell lines. These results suggest possible mechanisms and processes involved in the cytotoxic response of tumor cells to flavopiridol in addition to potential molecular markers that may serve as indicators of drug action.

## Materials and Methods

### Cell Culture and Treatment

The human tumor cell lines used in this study were PC3 (prostate carcinoma), DU145 (prostate carcinoma), U251 (glioma), and SF539 (glioma), which were obtained from American Type Culture Collection (Manassas, VA). Each cell line was grown in RPMI 1640 (Invitrogen, Carlsbad, CA) containing 5 mmol/L glutamate and 5% fetal bovine serum and maintained at 37°C in an atmosphere of 5% $CO_2$ and 95% room air. Flavopiridol, which was provided by the Division of Cancer Treatment and Diagnosis of the National Cancer Institute, was dissolved in DMSO to a stock concentration of 10 mmol/L, aliquoted, and stored at −20°C until use. Control samples received corresponding volumes of DMSO.

### Clonogenic Survival

Cultures were trypsinized to generate a single cell suspension, and a specified number of cells were seeded into each well of a six-well tissue culture plate. After allowing 6 hours for cells to attach, flavopiridol or DMSO (vehicle control) was added to the culture medium for 24 hours; the cultures were rinsed and fresh growth medium was added. Twelve to 14 days after seeding, colonies were stained with crystal violet, the number of colonies containing at least 50 cells was determined, and surviving fractions were calculated.

### RNA Sample Preparation and Probes Labeling

Cells were grown in 150-$mm^2$ tissue culture dishes and treated during exponential growth. Cells were exposed to increasing concentrations of flavopiridol (30 to 900 nmol/L) for 3 to 24 hours. Total RNA was extracted from each culture using TRIzol reagent (Invitrogen) passed through a RNeasy spin column (Qiagen, Valencia, CA) and amplified using RiboAmp RNA kit (Arcturus, Mountain View, CA) according to manufacturer's protocol. Amplified RNA (1.5 to 3.0 μg) was labeled with Cy5-dUTP (experimental RNA) or Cy3-dUTP (universal reference RNA, Stratagene, La Jolla, CA) using SuperScript II reverse transcriptase (Invitrogen).

### Microarray Procedure

Each cDNA microarray chip contained 7,680 human cDNA clones (NCI ROSP 8K Human Array), and methods for microarray hybridization and washing were described previously (17). Test sample RNAs from all flavopiridol-treated and untreated cells (vehicle DMSO) were competitively hybridized with the universal reference RNA mentioned above. Hybridized arrays were scanned with 10 μm resolution on a GenePix 4000A scanner (Axon Instruments, Inc., Foster City, CA) at wavelengths 635 and 532 nm for Cy5- and Cy3-labeled probes, respectively. The resulting TIFF images were analyzed by GenePix Pro 4.0 software (Axon Instruments). The ratios of the sample intensity to the reference red (Cy5)/green (Cy3) intensity for all targets were determined and ratio normalization was performed to normalize the center of ratio distribution to 1.0.

### Data Analysis

Raw intensity profiles were analyzed using the mAdb tools (Center for Information Technology, NIH) to perform microarray normalization and statistical analysis. All non-flagged raw fluorescent intensities were subjected to a spot quality filter with signal: background ratios >2, a minimum background corrected signal of 250 counts, and 60% of pixels in the spots with an intensity of >1 SD plus background. Outlier genes were extracted with ratios >2 or <0.5 in 100% of the microarrays. Hierarchical clustering was performed using a noncentered metric Pearson correlation. Each row represents data from a single cDNA microarray spot, while each column is a single experiment comparing two populations of treated and untreated cells. Red indicates that the gene is expressed >2-fold in the treated versus untreated cells, green indicates that the gene is expressed >2-fold in the untreated versus treated cells, and black indicates no difference between spot intensities of the treated and untreated cells.

### Real-time PCR

Eleven representative genes (*ABL1*, *BUB1*, *DKK1*, *FADD*, *MYC*, *RAD51*, *SMARCD2*, *TAF5L*, *TAF7*, *ZNF146*, and *CD99*), the expressions of which were commonly altered in all four cells treated with lethal dose of flavopiridol, were selected for quantitative analysis with real-time PCR. Total RNAs were reverse transcribed to single-stranded cDNAs using oligo(dT)12-18 primer with SuperScript II reverse transcriptase. Each cDNA was diluted for subsequent PCR amplification by monitoring *ACTB* as a quantitative control, an endogenous gene not affected by the concentrations of flavopiridol used in this study. Each PCR was carried out in a 12.5 μL volume for 5 minutes at 94°C for initial denaturing followed by 50 cycles of 94°C for 30 seconds and 60°C for 10 minutes in the Option 2 system (MJ Research, Waltham, MA).

## Results

To define the sensitivity of PC3 cells (human prostate carcinoma) to flavopiridol and to establish a clinically relevant biological endpoint for comparison with gene expression, clonogenic survival analysis was performed. This survival assay reflects all forms of cell death and can be used as a general indicator of flavopiridol-induced

cytotoxicity. Cells were exposed to specified concentrations of flavopiridol for 24 hours and were rinsed and fresh medium was added. Colonies were determined 12 to 14 days later. As shown in Fig. 1, flavopiridol exposure resulted in a concentration-dependent decrease in PC3 survival, consistent with the cytotoxicity reported in previous studies (1). It should be noted that flow cytometry performed on propidium iodide–stained cells did not detect a significant sub-$G_1$ population at any of the flavopiridol concentrations (data not shown). The level of apoptosis was also confirmed using FITC-labeled Annexin V (data not shown). These results indicate that the cell death induced by flavopiridol cannot be attributed to apoptosis.

To determine whether the cell death induced by flavopiridol resulted in a corresponding modification of gene expression in PC3 cells, microarray analysis was performed as a function of drug concentration and exposure time. As shown in Fig. 2A, at each concentration tested, as the flavopiridol exposure period increased, the number of genes with expression modified by >2-fold also increased. Likewise, at each time point evaluated, an increase in flavopiridol concentration was accompanied by an increase in the number of genes with modified expression. These data indicate that the flavopiridol-induced modification in gene expression was both concentration and time dependent.

As an initial investigation into a potential relationship between the cytotoxicity induced by flavopiridol (Fig. 1) and the modification in gene expression, a hierarchical cluster analysis was performed for each drug concentration at the 24-hour exposure point (Fig. 2B). The cluster analyses revealed a distinct difference in the modifications in gene expression induced by concentrations that killed ≥90% of the PC3 cells (300 and 900 nmol/L) and those flavopiridol concentrations that resulted in ≤50% cell killing. For example, the group of genes in subclusters A-C (Fig. 2B) denotes those genes that were down-regulated at the lethal concentrations (900 and 300 nmol/L) of flavopiridol but actually slightly up-regulated at the nonlethal concentrations (30, 60, and 90 nmol/L). Subclusters D and E (Fig. 2B) denote genes that were up-regulated by the lethal treatment of flavopiridol and unaffected or slightly down-regulated by the nonlethal treatment. This apparent relationship between changes in gene expression and lethality suggested that there is a transcriptome or gene expression profile indicative of flavopiridol-induced PC3 cell death.

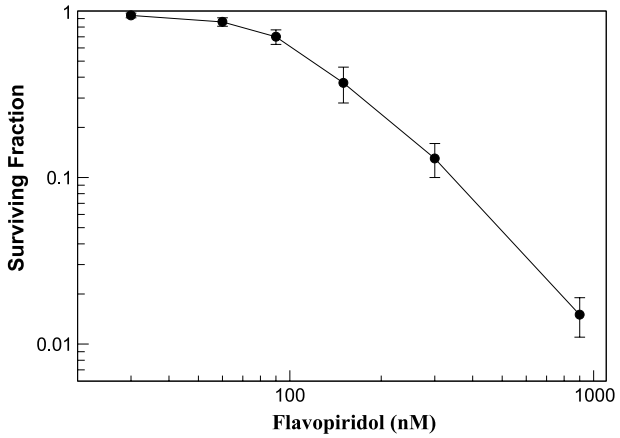


**Figure 1.** The effects of flavopiridol on PC3 cell survival. Cultures were trypsinized to generate a single cell suspension, and a specified number of cells were seeded into each well of a six-well tissue culture plate. After allowing 6 hours for cells to attach, flavopiridol or DMSO (vehicle control) was added to the culture medium for 24 hours; the cultures were rinsed and fresh growth medium was added. Colonies were determined 12 days later, and survival curves were generated. *Points,* means of three independent experiments; *bars,* SE.

To determine whether this putative death transcriptome was specific to PC3 cells or to prostate carcinoma cells in general, these studies were extended to the human tumor cell line DU145 (prostate carcinoma) and the two human glioma cell lines U251 and SF539. Exposure of each of the cell lines to flavopiridol (24 hours) resulted in a concentration-dependent decrease in clonogenic survival with 10% survival (90% cell death) corresponding to 600, 500, and 400 nmol/L for DU145, U251, and SF539, respectively (Fig. 3A). Microarray analysis was performed on these three cell lines after treatment with DMSO (vehicle control) and the concentration of flavopiridol corresponding to 90% cell death. The gene expression data were analyzed in combination with those generated from PC3 cells.

Microarray analysis of each of the four untreated (vehicle only) cell lines revealed relatively distinct gene expression profiles. The heterogeneity in gene expression was illustrated by comparing the microarray data sets generated for each of the untreated cell lines with each other via scatter plots (data not shown), which resulted in Pearson coefficients ranging from 0.277 to 0.575 with a corresponding range of outlier genes of 718 to 1,028. This is in contrast to comparing two data sets generated from the same untreated cell line, which results in Pearson coefficients of >0.90 with <20 outliers (data not shown). The heterogeneity in gene expression among the cell lines used in this study suggested that any common changes detected after flavopiridol exposure could be associated with the cytotoxic response to this antineoplastic agent.

Analysis of the flavopiridol-induced changes in gene expression revealed 798, 2,109, 1,816, and 1,240 genes for PC3, DU145, SF359, and U251 cells, respectively, which were either up-regulated or down-regulated by >2-fold compared with their respective vehicle-treated controls. Cluster analyses of the four cell lines indicated that exposure to a lethal concentration of flavopiridol resulted in gene expression profiles that were more similar than the profiles of the untreated cells. This relative general modification is illustrated by the dendrogram in Fig. 3B, which uses Euclidean distance to represent degrees of similarity/disparity (18). The scale at the top of the dendrogram depicts the correlation coefficient of the outlier gene patterns, which corresponds to the length of the dendrogram

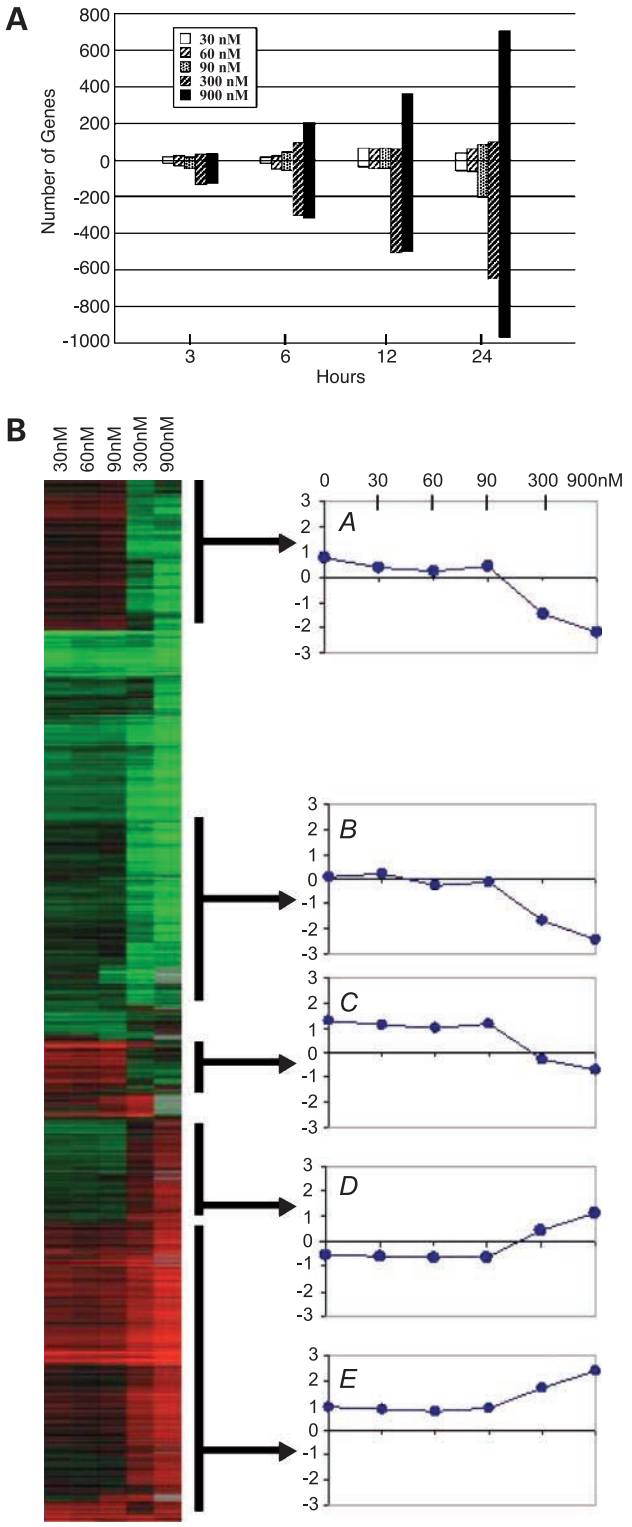


**Figure 2.** Hierarchical clustering of gene expression in PC3 cells as a function of flavopiridol concentration. **A** and **B,** increased expression (*red*) and decreased expression (*green*) in flavopiridol-treated cells as compared with vehicle-treated cells. **B,** *black box,* no difference in expression; *gray boxes,* missing data. *Right,* a graphical depiction of the gene expression changes within specified subclusters (*A-E*).

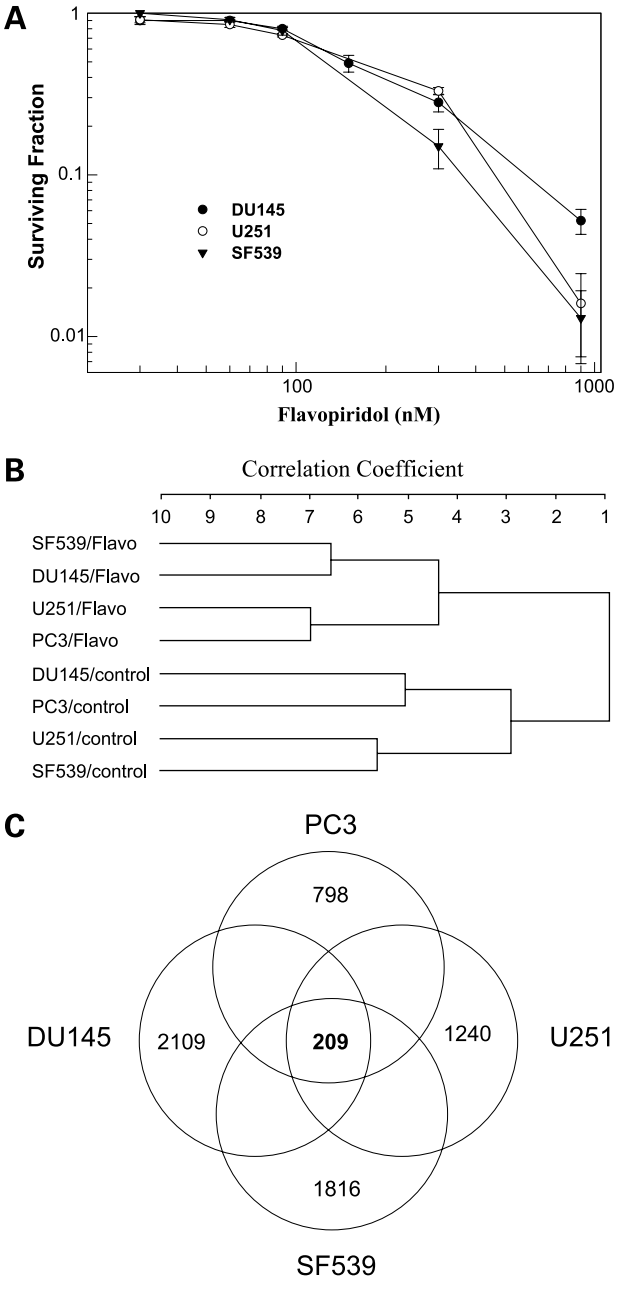


**Figure 3.** The effects of flavopiridol on DU145, U251, and SF539 cell survival. **A,** cultures were trypsinized to generate a single cell suspension, and a specified number of cells were seeded into each well of a six-well tissue culture plate. After allowing 6 hours for cells to attach, flavopiridol or DMSO (vehicle control) was added to the culture medium for 24 hours; the cultures were rinsed and fresh growth medium was added. Colonies were determined 12 to 14 days later, and survival curves were generated. *Points,* means of three independent experiments; *bars,* SE. **B,** dendrogram comparing the correlation coefficients for control and flavopiridol-treated cells. The flavopiridol treatment of SF539, DU145, U251, and PC3 cells was for 24 hours at 400, 600, 500, and 300 nmol/L, respectively. The controls were exposed to corresponding volumes of DMSO. **C,** graphical representation of the number of outliers for each cell line and the common outliers found in the group of four cell lines.

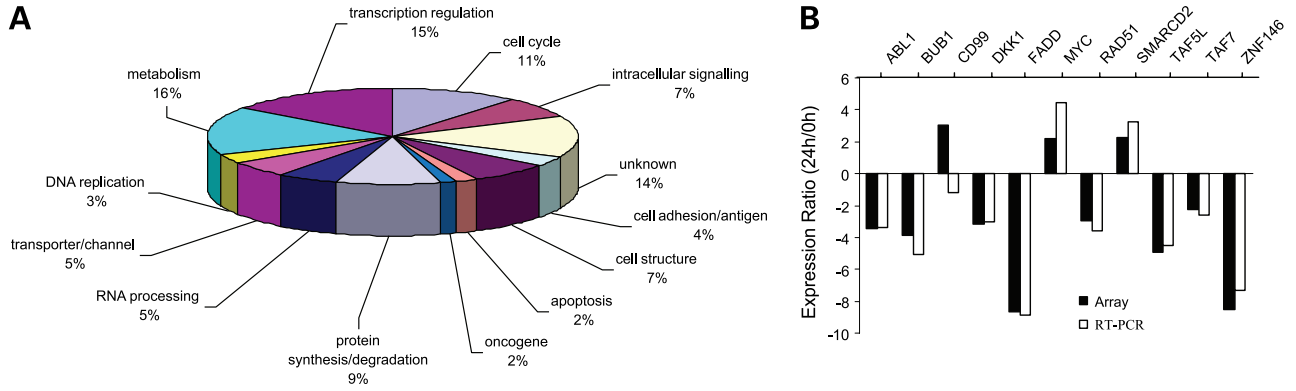


**Figure 4.** Functional classification and verification of the death transcriptome genes. **A,** this pie chart represents the Kyoto Encyclopedia of Genes and Genomes pathway classification of gene functions in the 209 gene transcriptome. **B,** comparison of gene expression as determined by microarray analysis and real-time PCR. The expression ratios between 24 hours of flavopiridol treatment and vehicle control for PC3 cells were compared for 11 selected genes. *Columns,* average of three independent real-time PCR reactions and duplicate microarray slides.

branches connecting pairs of nodes. According to this model, as two cell lines are more dissimilar, the branch point occurs at a further distance from the branch source. As shown in Fig. 3B, the branch point for each of the cell lines exposed to flavopiridol was closer to the branch source than for the untreated cells. Thus, analysis of the entire microarray data set suggests that flavopiridol reduces the heterogeneity in gene expression between the cell lines.

Moreover, comparison of the individual genes affected in each of the cell lines by flavopiridol exposure resulted in the identification of a set of 209 genes (common outliers), with modified expression in each of the cell lines (Fig. 3C). This set of 209 common outliers in flavopiridol-treated cells included 185 down-regulated and 21 up-regulated genes with ranges of 2.01- to 62.2-fold for down-regulated and 2.02- to 20.22-fold for up-regulated. The genes commonly affected by flavopiridol are diverse in their putative functions including regulation of cell cycle, signal transduction, DNA repair, transcription, cell adhesion, cell structure, and apoptosis (Fig. 4A). Each gene, its accession number, description, fold change over control treated cells, and functional class are listed in Table 1. Validation of these changes in expression detected by microarray analysis was performed on a subset of 11 genes in each cell line using real-time PCR. The modifications in expression of the 11 genes in PC3 cells after flavopiridol exposure as determined by real-time PCR and microarray analysis are shown in Fig. 4B. Of the 11 changes predicted by microarray analysis, 10 were also detected by real-time PCR. The same relative changes were obtained for the other cell lines (data not shown).

## Discussion

Recent approaches to cancer treatment have emphasized the development of agents directed against a molecule critical to tumor cell survival. A frequently cited example of this targeted-directed approach is the use of Gleevec for the treatment of chronic myelogenous leukemia (19). However, whereas there has been some success in the treatment of hematopoietic neoplasms, the use of targeted chemotherapy in the treatment of solid tumors has, for the most part, not been as successful. Potential reasons for the resistance of solid tumor cells to targeted therapy include the existence of redundant survival pathways and the presence of multiple, nonclonal tumor subpopulations. Moreover, in response to a cytotoxic insult, solid tumor cells generally undergo a nonapoptotic form of death, which has not been well described at the molecular level. A more effective strategy for therapy of solid tumors may involve an agent that targets more than one survival pathway or critical molecule. Although initially developed as a cdk inhibitor, flavopiridol appears to have multiple targets within a tumor cell, known and unknown (20). Defining the processes occurring during flavopiridol-induced cytotoxicity may not only contribute to the understanding of the mechanisms of drug action but also provide insight into the processes involved in nonapoptotic cell death in general. Moreover, such information may lead to the identification of molecular markers indicative of flavopiridol action, which would be of benefit in clinical applications. Toward this end, we have used microarray analysis to define the genes with modified expression after exposure of solid tumor cell lines to cytotoxic flavopiridol concentrations.

The data presented indicate that flavopiridol-induced death was accompanied by a wide range in gene expression changes among the two prostate carcinomas and two gliomas evaluated ranging from 728 to 2,109 outlier genes. However, of interest, there was a common set of 209 genes that were affected in each of the solid tumor cell lines. Because the gene expression profiles of the untreated cells were quite distinct, the changes detected in the same 209 genes in each of the cell lines were unlikely the result of chance and could be attributed to flavopiridol treatment. Moreover, these changes were not detected after exposure to flavopiridol concentrations that resulted in <50% cell

**Table 1. Gene expression changes detected in PC3, DU145, SF359, and U251 cells treated with flavopiridol**

| Accession | Symbol | Description | Fold Difference* | | | |
|---|---|---|---|---|---|---|
| | | | PC3 | DU145 | SF359 | U251 |
| | | | 300 nmol/L | 600 nmol/L | 400 nmol/L | 500 nmol/L |
| | | *Regulation of cell cycle* | | | | |
| X16416 | *ABL1* | Abl tyrosine-protein kinase | −3.45 | −2.13 | −5.44 | −8.13 |
| AA071486 | *AURKB* | Aurora kinase B | −2.74 | −7.09 | −5.00 | −5.14 |
| AF043294 | *BUB1* | Putative mitotic checkpoint protein serine/threonine kinase | −3.84 | −4.19 | −19.65 | −3.84 |
| AA774665 | *CCNB2* | Cyclin B2 | −3.34 | −9.19 | −18.88 | −3.65 |
| AA598974 | *CDC2* | Cell division cycle 2, $G_1$-S and $G_2$-M | −2.97 | −7.28 | −13.36 | −2.07 |
| R20737 | *CDC23* | Cell division cycle 23, yeast homologue | −3.65 | −4.18 | −5.70 | −3.50 |
| AA213816 | *CDC42EP3* | CDC42 effector protein (Rho GTPase binding) 3 | −3.36 | −2.79 | −2.54 | −2.65 |
| N74285 | *CDC5L* | Cell division cycle 5 like (*Schizosaccharomyces pombe*) | −5.61 | −11.42 | −7.41 | −2.97 |
| X77743 | *CDK7* | Complexes with cyclin H to form a component of *TFIIH* | −2.30 | −2.68 | −2.35 | −2.82 |
| R59679 | *CDK8* | Cyclin-dependent kinase 8 | −6.00 | −2.18 | −2.46 | −3.68 |
| AA397813 | *CKS2* | CDC28 protein kinase regulatory subunit 2 | −3.19 | −8.54 | −13.86 | −9.80 |
| AA052960 | *DKC1* | Dyskeratosis congenita 1, dyskerin | −2.11 | −5.73 | −6.11 | −4.01 |
| AA677396 | *DNAJA2* | DnaJ (Hsp40) homologue, subfamily A, member 2 | −4.82 | −3.57 | −3.67 | −7.58 |
| AA430503 | *KIF22* | Kinesin family member 22 | −2.39 | −2.01 | −5.10 | − 4.51 |
| AA676460 | *KPNA2* | Karyopherin α2 | −4.52 | −17.48 | −11.08 | −9.06 |
| AA478525 | *MPHOSPH6* | M-phase phosphoprotein 6 | −2.38 | −7.07 | −4.59 | −3.12 |
| N50584 | *NOL1* | Nucleolar protein 1 | −2.45 | −3.46 | −2.47 | −2.43 |
| J04718 | *PCNA* | Proliferating cell nuclear antigen | −7.83 | −11.61 | −13.21 | −13.99 |
| R26732 | *PMP22* | Peripheral myelin protein 22 | −3.26 | −4.57 | −10.39 | −11.48 |
| AA418821 | *STRN3* | Striatin, calmodulin binding protein 3 | −4.19 | −2.57 | −2.75 | −2.63 |
| AA775806 | *WDR3* | WD repeat domain 3 | −6.40 | −9.34 | −9.61 | −4.70 |
| | | *Cell signal transduction* | | | | |
| AA012867 | *ARF6* | ADP-ribosylation factor 6 | −7.40 | −20.70 | −13.59 | −8.71 |
| H70464 | *ARHGAP4* | Rho GTPase activating protein 4 | −2.08 | −5.01 | −5.65 | −2.29 |
| R44288 | *CALM2* | Calmodulin 2 (phosphorylase kinase δ) | −3.48 | −25.24 | −10.59 | −5.38 |
| AA253464 | *DKK1* | Dickkopf homologue 1 (*Xenopus laevis*) | −3.41 | −62.21 | −2.10 | −40.89 |
| AA676885 | *MAP2K1IP1* | Mitogen-activated protein kinase kinase 1 interacting protein 1 | −3.07 | −5.36 | −5.29 | −7.55 |
| X80692 | *MAPK6* | Mitogen-activated protein kinase 6 | −5.91 | −4.14 | −8.48 | −6.68 |
| AA778230 | *MAPKAPK5* | Mitogen-activated protein kinase-activated protein kinase 5 | −3.01 | −2.86 | −4.49 | −4.00 |
| AA158244 | *RGS12* | Regulator of G-protein signaling 12 | −4.24 | −5.24 | −4.24 | −3.99 |
| AF024636 | *STK24* | Ste20-like kinase 3 (mst-3) | −3.11 | −2.39 | −5.55 | −4.16 |
| AA521346 | *STK38* | Serine/threonine kinase 38 | −3.03 | −3.15 | −3.66 | −2.35 |
| AA134814 | *TANK* | TRAF family member-associated nuclear factor-κB activator | −2.10 | −2.65 | −4.61 | −2.91 |
| AA504459 | *TRRAP* | Transformation/transcription domain-associated protein | −2.35 | −4.17 | −3.20 | −3.21 |
| AA451895 | *ANXA5* | Annexin A5 | 2.24 | 0.68 | 2.73 | 3.15 |

NOTE: Cultures were exposed to the designated flavopiridol concentration for 24 hours, which was sufficient to reduce survival to 10% as determined by a colony-forming assay. Expressed sequence tags, hypothetical and unknown proteins: AA194246, N62460, AA496804, AA779416, AA455882, AI651167, AA663941, H99695, AA150301, AA432056, AA465242, AA496002, AA490991, R45977, AA630449, AA489232, AA489080, AA863469, AA708955, AA191426, AA425020, R60847, U69668, AA455970, and AA115537 (25).

*The fold difference in expression levels of the individual genes was determined based on the comparison with corresponding cultures exposed to DMSO (vehicle control). A negative value refers to a decrease in relative expression, and a positive value refers to an increase in relative expression.

*(Continued on following page)*

**Table 1. Gene expression changes detected in PC3, DU145, SF359, and U251 cells treated with flavopiridol (Cont'd)**

| Accession | Symbol | Description | Fold Difference* | | | |
|---|---|---|---|---|---|---|
| | | | PC3 | DU145 | SF359 | U251 |
| | | | 300 nmol/L | 600 nmol/L | 400 nmol/L | 500 nmol/L |
| | | *DNA repair* | | | | |
| AA609609 | *ALKBH* | AlkB, alkylation repair homologue (*Escherichia coli*) | −2.62 | −2.04 | −2.05 | −2.74 |
| AA478273 | *APEX1* | APEX nuclease 1 | −2.81 | −7.46 | −4.22 | −2.16 |
| AA010492 | *MBD4* | Methyl-CpG binding domain protein 4 | −5.59 | −6.02 | −8.29 | −2.14 |
| AF058392 | *RAD1* | Hrad1, cell cycle checkpoint protein | −5.18 | −5.93 | −3.00 | −3.07 |
| AA873056 | *RAD51* | *RAD51* homologue (RecA homologue, *E. coli*) | −2.93 | −5.28 | −5.42 | −3.03 |
| AB036063 | *RRM2B* | p53R2, p53-inducible nuclear ribonucleotide reductase | −2.72 | −2.43 | −4.20 | −2.47 |
| U51166 | *TDG* | G/T mismatch-specific thymine DNA glycosylase | −4.61 | −3.35 | −2.88 | −2.09 |
| | | *Regulation of transcription* | | | | |
| U51432 | *SNW1* | Skip, ski oncogene interacting nuclear protein | −4.14 | −3.32 | −8.31 | −2.73 |
| AA029042 | *SIAH2* | Seven in absentia homologue 2 (*Drosophila*) | −2.07 | −2.24 | −10.40 | −4.22 |
| X12795 | *CBF2* | COUP transcription factor, group F, member 1 | −2.74 | −2.71 | −3.10 | −5.39 |
| W72437 | *GTF2H2* | General transcription factor IIH polypeptide 2 | −6.28 | −7.47 | −4.26 | −2.19 |
| AA922691 | *GTF3C2* | General transcription factor IIIC polypeptide 2 | −3.07 | −5.64 | −4.35 | −3.00 |
| AA935533 | *E2F6* | E2F transcription factor 6 | −3.33 | −2.81 | −3.57 | −4.31 |
| M96426 | *TIAL1* | TIAR, nucleolysin | −4.20 | −4.06 | −3.49 | −2.00 |
| AA063580 | *TAF7* | *TAF7* RNA polymerase II, TATA box binding protein-associated factor | −2.27 | −4.41 | −8.48 | −4.74 |
| AA447793 | *PURA* | Purine-rich element binding protein A | −6.21 | −4.54 | −3.55 | −2.56 |
| AA055932 | *TAF5L* | TAF5-like RNA polymerase II | −4.90 | −2.94 | −5.81 | −2.44 |
| AF119042 | *TIF1* | Transcriptional intermediary factor 1 | −3.96 | −4.38 | −5.40 | −3.84 |
| AA480876 | *ABT1* | Activator of basal transcription 1 | −2.83 | −2.46 | −2.59 | −5.13 |
| L41067 | *NFATC3* | Nuclear factor of activated T-cells, cytoplasmic, calcineurin-dependent 3 | −2.34 | −3.51 | −3.86 | −2.59 |
| AA479052 | *POLR2A* | Polymerase (RNA) II polypeptide A | −2.86 | −3.47 | −2.31 | −2.03 |
| AA629687 | *NFE2L2* | Nuclear factor (erythroid-derived 2)-like 2 | −2.32 | −3.77 | −6.91 | −4.89 |
| AA629686 | *EED* | Embryonic ectoderm development | −2.27 | −10.71 | −5.39 | −5.85 |
| X52560 | *CEBP* | NF-IL6, CAAT/enhancer binding protein-β | −2.44 | −2.11 | −5.72 | −17.63 |
| AA487115 | *IVNS1ABP* | Influenza virus NS1A binding protein | −2.19 | −5.46 | −3.10 | −2.01 |
| AA704187 | *PLAGL2* | Pleiomorphic adenoma gene-like 2 | −3.04 | −2.21 | −3.20 | −4.39 |
| AA418544 | *NR2F2* | Nuclear receptor subfamily 2, group F, member 2 | −2.45 | −4.81 | −6.42 | −9.12 |
| W88740 | *COIL* | Coilin | −3.25 | −2.07 | −5.46 | −6.77 |
| AA416783 | *RBPSUH* | Recombining binding protein suppressor of hairless | −3.78 | −4.79 | −5.61 | −2.47 |
| AA977080 | *WHSC2* | Wolf-Hirschhorn syndrome candidate 2 | −2.42 | −4.60 | −2.21 | −4.72 |
| AA456439 | *MADH4* | MAD, mothers against decapentaplegic homologue 4 (*Drosophila*) | −2.66 | −4.16 | −11.28 | −5.63 |
| AA894577 | *NOL5A* | Nucleolar protein 5A | −3.13 | −2.97 | −3.03 | −3.04 |
| U32849 | *NMI* | Interleukin-2 and IFN-γ-inducible potentiator of STAT-induced transcription | −4.06 | −9.30 | −12.23 | −2.17 |
| AI675929 | *ZNF239* | Zinc finger protein 239 | −2.59 | −3.02 | −2.96 | −3.47 |
| R26082 | *ZNF354A* | Zinc finger protein 354A | −2.44 | −2.47 | −2.68 | −2.39 |
| AA455657 | *ZNF184* | Zinc finger protein 184 (Kruppel-like) | −2.83 | −5.35 | −2.80 | −2.47 |
| N59119 | *ZNF207* | Zinc finger protein 207 | −4.08 | −9.25 | −11.50 | −3.86 |
| AA504351 | *ZNF146* | Zinc finger protein 146 | −8.50 | −8.94 | −6.89 | −4.50 |
| AA252169 | *ZNF193* | Zinc finger protein 193 | −3.14 | −3.35 | −2.10 | −2.26 |
| V00568 | *MYC* | c-*myc* | 3.04 | 7.01 | 7.31 | 3.68 |
| AA478436 | *SMARCD2* | SWI/SNF related, matrix associated, actin-dependent regulator of chromatin, subfamily D, member 2 | 2.27 | 12.11 | 5.77 | 5.20 |

*(Continued on following page)*

**Table 1. Gene expression changes detected in PC3, DU145, SF359, and U251 cells treated with flavopiridol (Cont'd)**

| Accession | Symbol | Description | Fold Difference* | | | |
|---|---|---|---|---|---|---|
| | | | PC3 | DU145 | SF359 | U251 |
| | | | 300 nmol/L | 600 nmol/L | 400 nmol/L | 500 nmol/L |
| | | *Cell adhesion and surface antigen* | | | | |
| H19687 | *APBA1* | Amyloid precursor protein binding, family A, member 1 | −2.23 | −2.89 | −3.93 | −2.32 |
| Y00636 | *CD58* | LFA-3 | −2.60 | −2.02 | −5.17 | −4.72 |
| AA425302 | *MAGEF1* | Melanoma antigen family F1 | −7.70 | −18.58 | −16.90 | −15.64 |
| AA449715 | *SRPX* | Sushi repeat-containing protein, X-linked | 2.22 | 4.72 | 2.69 | 2.36 |
| AA937895 | *CD99* | *CD99* antigen | 2.17 | 2.22 | 3.59 | 2.13 |
| M11886 | *HLA-C* | MHC class I, HLA-C4 | 2.29 | 2.22 | 3.76 | 2.40 |
| AA670408 | *B2M* | β2-microglobulin | 2.48 | 7.77 | 2.42 | 2.77 |
| | | *Cell structure* | | | | |
| AA644128 | *NASP* | Nuclear autoantigenic sperm protein | −2.01 | −2.13 | −3.82 | −3.36 |
| AA888148 | *TUBB2* | Tubulin β2 | −3.43 | −5.37 | −7.14 | −8.52 |
| AA496787 | *COL9A3* | Collagen, type IX α3 | −2.18 | −3.16 | −3.98 | −2.47 |
| AA608514 | *H3F3B* | H3 histone family 3B | −4.31 | −8.08 | −3.25 | 13.45 |
| AA504625 | *KIF11* | Kinesin family member 11 | −4.59 | −3.39 | −24.76 | −13.82 |
| NM_004856 | *KIF23* | Kinesin family member 23 | −3.35 | −9.15 | −12.23 | −4.28 |
| N54552 | *TUBGCP3* | Tubulin γ complex associated protein 3 | −7.00 | −4.96 | −3.77 | −3.67 |
| AA629558 | *SLBP* | Stem-loop (histone) binding protein | −2.89 | −21.19 | −9.95 | −8.75 |
| AA701455 | *CENPF* | Centromere protein F, 350/400ka (mitosin) | −5.43 | −3.97 | −7.72 | −7.31 |
| AW081868 | *TUBB* | Tubulin β polypeptide | −4.28 | −7.42 | −2.44 | −5.11 |
| H06295 | *HIST2H2BE* | Histone 2, H2be | 2.54 | 2.34 | 4.01 | 5.82 |
| AA278759 | *PRG1* | Proteoglycan 1 secretory granule | 2.02 | 8.47 | 2.38 | 3.18 |
| N21079 | *HSA6591* | Nucleolar cysteine-rich protein | −4.25 | −6.38 | −4.45 | −2.77 |
| AA733061 | *NUP54* | Nucleoporin 54 kDa | −3.10 | −3.93 | −7.32 | −3.25 |
| N72193 | *CETN2* | Centrin, EF-hand protein, 2 | 2.33 | 2.20 | 3.84 | 4.95 |
| | | *Apoptosis* | | | | |
| N62514 | *BNIP2* | BCL2/adenovirus E1B interacting protein 2 | −2.42 | −3.13 | −8.97 | −3.77 |
| U24231 | *FADD* | MORT | −8.63 | −16.02 | −5.50 | −15.16 |
| N33236 | *MRPS30* | Mitochondrial ribosomal protein S30 | −6.89 | −15.01 | −7.27 | −5.32 |
| AA775261 | *PDCD6* | Programmed cell death 6 | −2.36 | −9.00 | −5.30 | −2.58 |
| | | *Oncogene* | | | | |
| H98543 | *RAB9A* | Member RAS oncogene family | −2.64 | −2.00 | −3.04 | −4.71 |
| N69689 | *RAB1A* | Member RAS oncogene family | −2.48 | −20.10 | −5.96 | −3.68 |
| AA134570 | *RAB23* | Member RAS oncogene family | −6.14 | −3.43 | −10.38 | −3.53 |
| | | *Receptor* | | | | |
| AA476490 | *TRIP4* | Thyroid hormone receptor interactor 4 | −2.78 | −2.30 | −6.70 | −2.63 |
| AA 047567 | *PGRMC2* | Progesterone receptor membrane component 2 | −2.89 | −3.28 | −4.57 | −4.00 |
| N30573 | *NRBF-2* | Nuclear receptor binding factor-2 | −4.40 | −4.94 | −5.68 | −6.68 |
| | | *Protein synthesis/degradation* | | | | |
| R66383 | *CLPX* | Caseinolytic protease X homologue (*E. coli*) | −5.56 | −6.53 | −5.53 | −3.50 |
| AA487235 | *FBXO11* | F-box only protein 11 | −2.25 | −3.21 | −2.39 | −2.82 |
| AA460305 | *DDX20* | DEAD (Asp-Glu-Ala-Asp) box polypeptide 20 | −3.95 | −3.46 | −4.05 | −6.25 |
| N79030 | *DDX48* | DEAD (Asp-Glu-Ala-Asp) box polypeptide 48 | −3.01 | −9.13 | −14.01 | −4.25 |
| AA461476 | *DDX56* | DEAD (Asp-Glu-Ala-Asp) box polypeptide 56 | −6.78 | −11.92 | −3.84 | −5.53 |
| AA278698 | *FAM16AX* | Family with sequence similarity 16, member A, X-linked | −4.02 | −4.51 | −3.35 | −5.06 |
| AA419143 | *JTV1* | *JTV1* gene | −5.21 | −9.53 | −16.72 | −7.40 |
| AA404286 | *PPIF* | Peptidylprolyl isomerase F | −2.07 | −2.93 | −4.26 | −3.11 |

*(Continued on following page)*

**Table 1. Gene expression changes detected in PC3, DU145, SF359, and U251 cells treated with flavopiridol (Cont'd)**

| Accession | Symbol | Description | Fold Difference* | | | |
|---|---|---|---|---|---|---|
| | | | PC3 | DU145 | SF359 | U251 |
| | | | 300 nmol/L | 600 nmol/L | 400 nmol/L | 500 nmol/L |
| AA598492 | *UBE2B* | Ubiquitin-conjugating enzyme E2B (RAD6 homologue) | −2.49 | −2.43 | −3.24 | −3.87 |
| AA430504 | *UBE2C* | Ubiquitin-conjugating enzyme E2C | −2.91 | −2.01 | −13.94 | −4.94 |
| AA621256 | *SUSP1* | SUMO-1-specific protease | −3.90 | −3.30 | −5.73 | −2.33 |
| AA424503 | *PSMC6* | Proteasome 26S subunit, ATPase 6 | −4.29 | −9.23 | −12.52 | −6.50 |
| AA455652 | *RARS* | Arginyl-tRNA synthetase | −2.05 | −2.86 | −9.37 | −2.50 |
| N62725 | *UBQLN2* | Ubiquilin 2 | −2.69 | −3.63 | −8.03 | −2.68 |
| AI969221 | *RPL41* | Ribosomal protein L41 | 2.03 | 2.77 | 2.92 | 2.55 |
| AI951501 | *RPL12* | Ribosomal protein L12 | 2.30 | 2.68 | 3.27 | 3.11 |
| | | *RNA processing* | | | | |
| AA701981 | *C2F* | C2f protein | −2.72 | −6.10 | −8.94 | −3.96 |
| AA703250 | *PRPF4* | PRP4 pre-mRNA processing factor 4 homologue (yeast) | −3.74 | −2.80 | −3.03 | −3.83 |
| H11720 | *SFRS10* | Splicing factor, arginine/serine-rich 10 | −2.01 | −5.13 | −4.15 | −2.25 |
| AA598400 | *SFRS3* | Splicing factor, arginine/serine-rich 3 | −2.51 | −4.06 | −8.95 | −7.55 |
| AA454585 | *SFRS2* | Splicing factor, arginine/serine-rich 2 | −2.45 | −9.60 | −3.50 | −3.55 |
| AA708261 | *LSM6* | LSM6 homologue (*Saccharomyces cerevisiae*) | −2.32 | −5.34 | −12.53 | −3.34 |
| AA293218 | *CSTF2* | Cleavage stimulation factor, 3′ pre-RNA, subunit 2, 64 kDa | −2.63 | −2.24 | −4.13 | −2.07 |
| AA411407 | *SRP19* | Signal recognition particle | −5.20 | −4.49 | −10.23 | −2.29 |
| AA122272 | *SNRPA1* | Small nuclear ribonucleoprotein polypeptide A′ | −2.59 | −12.14 | −9.21 | −2.81 |
| H78385 | *HIP2* | Huntingtin interacting protein 2 | −3.10 | −9.43 | −8.00 | −2.04 |
| | | *Transporter/channel* | | | | |
| AA450205 | *TLOC1* | Translocation protein 1 | −4.84 | −5.06 | −11.86 | −2.40 |
| D87969 | *C6orf165* | CMP-sialic acid transporter member 1 | −5.92 | −4.49 | −3.09 | −2.24 |
| K03195 | *SLC2A1* | Glucose transporter (HepG2) | −2.47 | −3.87 | −6.15 | −10.92 |
| T59055 | *XPO1* | Exportin 1 (CRM1 homologue, yeast) | −2.65 | −3.02 | −2.89 | −2.36 |
| N62620 | *KCNK1* | Potassium channel, subfamily K, member 1 | −4.10 | −2.27 | −2.66 | −3.77 |
| AA521350 | *SEP15* | 15-kDa Selenoprotein | 2.25 | 4.25 | 2.49 | 2.89 |
| AA995093 | *NOLA1* | Nucleolar protein family A, member 1 | −3.40 | −5.80 | −3.89 | −2.47 |
| AA504128 | *RAE1* | RAE1 RNA export 1 homologue (*S. pombe*) | −2.72 | −5.33 | −8.86 | −2.04 |
| AA485958 | *HRB* | HIV-1 Rev binding protein | −2.47 | −5.00 | −3.06 | −2.13 |
| AA449107 | *SEC24D* | SEC24-related gene family, member D (*S. cerevisiae*) | −2.27 | −3.76 | −16.83 | −6.23 |
| | | *DNA replication* | | | | |
| H73714 | *RFC1* | Replication factor C (activator 1) 1 | −4.20 | −4.85 | −5.89 | −5.28 |
| N39611 | *RFC3* | Replication factor C (activator 1) 3 | −6.29 | −3.64 | −3.30 | −2.37 |
| M87339 | *RFC4* | Replication factor C (activator 1) 4 | −4.70 | −5.83 | −14.98 | −4.27 |
| R97785 | *TOPBP1* | Topoisomerase (DNA) II binding protein | −2.90 | −3.70 | −12.00 | −2.10 |
| AA504348 | *TOP2A* | Topoisomerase (DNA) IIα | −2.02 | −4.00 | −14.94 | −2.43 |
| AA670197 | *HMGB3* | High-mobility group box 3 | −3.61 | −5.47 | −3.82 | −4.79 |
| | | *Metabolism* | | | | |
| AA877194 | *ATP6V1B2* | ATPase V1 subunit B isoform 2 | −4.43 | −9.68 | −5.53 | −3.27 |
| N66208 | *PPP1R8* | Protein phosphatase 1 regulatory (inhibitor) subunit 8 | −4.89 | −2.94 | −18.36 | −13.92 |
| AA460981 | *GOLGA4* | Golgi autoantigen, golgin subfamily A4 | −3.38 | −2.91 | −3.93 | −2.17 |
| AA709044 | *ARFGAP3* | ADP-ribosylation factor GTPase activating protein 3 | −2.84 | −3.53 | −2.63 | −2.09 |
| AA431414 | *ADSS* | Adenylosuccinate synthase | −7.92 | −12.94 | −6.25 | −5.19 |

*(Continued on following page)*

**Table 1. Gene expression changes detected in PC3, DU145, SF359, and U251 cells treated with flavopiridol (Cont'd)**

| Accession | Symbol | Description | Fold Difference* | | | |
|---|---|---|---|---|---|---|
| | | | PC3 | DU145 | SF359 | U251 |
| | | | 300 nmol/L | 600 nmol/L | 400 nmol/L | 500 nmol/L |
| AA280846 | *CBR1* | Carbonyl reductase 1 | −2.29 | −5.69 | −5.01 | −2.16 |
| AA495802 | *HMBS* | Hydroxymethylbilane synthase | −2.01 | −5.12 | −5.25 | −6.22 |
| M87339 | *RFC4* | Replication factor C (activator 1) 4 | −4.70 | −5.83 | −14.98 | −4.27 |
| AF027302 | *ABCF1* | ATP binding cassette, subfamily F, member 1 | −3.50 | −4.51 | −5.65 | −3.81 |
| MN_002408 | *MGAT2* | Mannosyl (α-1,6-)-glycoprotein β-1,2-*N*-acetylglucosaminyltransferase | −2.49 | −12.46 | −4.41 | −4.05 |
| AA777551 | *MTHFS* | 5,10-Methenyltetrahydrofolate synthetase | −2.27 | −5.82 | −3.92 | −2.50 |
| AA417881 | *BLMH* | Bleomycin hydrolase | −4.82 | −4.75 | −2.28 | −2.91 |
| T59245 | *MAT2A* | Methionine adenosyltransferase IIα | −3.41 | −5.53 | −2.77 | −3.48 |
| AA446557 | *HUMAUANTIG* | Nucleolar GTPase | −2.40 | −2.46 | −4.68 | −2.52 |
| AA085749 | *APACD* | ATP binding protein associated with cell differentiation | −2.42 | −4.27 | −9.59 | −3.76 |
| AA007699 | *PIGC* | Phosphatidylinositol glycan class C | −5.30 | −2.67 | −4.29 | −7.28 |
| W69906 | *UMPK* | UMP kinase | −2.85 | −2.30 | −10.02 | −6.31 |
| AF400434 | *PAFAH1B1* | Platelet-activating factor acetylhydrolase isoform Ib | −2.87 | −3.15 | −3.40 | −3.27 |
| N64014 | *PIP5K1A* | Phosphatidylinositol-4-phosphate 5-kinase type Iα | −4.45 | −7.57 | −3.59 | −3.48 |
| AA463411 | *DDAH1* | Dimethylarginine dimethylaminohydrolase 1 | −4.50 | −4.14 | −15.20 | −4.26 |
| N52450 | *AADAT* | Aminoadipate aminotransferase | −2.17 | −4.39 | −2.42 | −2.01 |
| AA679468 | *PITPNB* | Phosphatidylinositol transfer protein β | −4.39 | −3.63 | −3.54 | −5.58 |
| R43634 | *BCAS2* | Breast carcinoma amplified sequence 2 | −3.19 | −8.14 | −5.51 | −2.14 |
| AA040861 | *UAP1* | UDP *N*-acetylglucosamine pyrophosphorylase 1 | −4.56 | −10.87 | −6.60 | −3.38 |
| AA126919 | *TPST1* | Tyrosylprotein sulfotransferase 1 | −2.89 | −5.27 | −4.83 | −2.77 |
| R43981 | *GOT1* | Glutamic-oxaloacetic transaminase 1 | −2.30 | −2.49 | −3.57 | −4.68 |
| AA873575 | *PPAT* | Phosphoribosyl pyrophosphate amidotransferase | −6.25 | −8.38 | −2.18 | −2.88 |
| U25182 | *PRDX4* | Thioredoxin peroxidase | 2.57 | 2.43 | 2.99 | 2.18 |
| AA629862 | *UQCR* | Ubiquinol-cytochrome c reductase subunit | 2.06 | 3.96 | 2.81 | 2.04 |
| H18938 | *ACY1* | Aminoacylase 1 | 3.15 | 20.22 | 2.72 | 3.05 |
| AW009090 | *NDUFB3* | NADH dehydrogenase (ubiquinone) 1β subcomplex 3 | 2.41 | 2.42 | 2.44 | 3.59 |
| AI362062 | *NOVA1* | Neuro-oncological ventral antigen 1 | 2.05 | 6.08 | 3.85 | 4.39 |

death. Thus, the identification of this common set of 209 gene expression changes suggests that flavopiridol-induced cell death can be defined in terms of a specific transcriptome.

With respect to the mode of cell death, the transcriptome generated after exposure to cytotoxic flavopiridol concentrations did not contain any proapoptotic genes. Moreover, a significant reduction in Fas-associated death domain expression was detected. Fas-associated death domain is a critical component of the apoptotic pathway mediated through Fas, which is activated after exposure to the certain chemotherapeutic agents including cisplatin, doxorubicin, and etoposide (21, 22). Inhibition of Fas-associated death domain activity using a dominant negative construct has been shown to reduce the amount of chemotherapy-induced apoptosis (23). In the four tumor cell lines used in this study, no significant apoptosis was detected after exposure to cytotoxic concentrations of flavopiridol. Thus, the death transcriptome identified for flavopiridol is consistent with a nonapoptotic process of cell death.

Of the 209 genes in the flavopiridol death transcriptome, the majority of changes (185) involved decreases in gene expression. This general decrease is consistent with the reduction of a series of transcription factors, 31 are down-regulated in our study including 6 zinc finger proteins. Many of these were down-regulated at an earlier 3-hour time point in PC3 cells (data not shown). Of potential interest are the decreases in CAAT/enhancer binding protein-β and E2F6. CAAT/enhancer binding protein-β regulates the expression of a variety of genes involved in the integration of cellular metabolic processes (24). In addition, CAAT/enhancer binding protein-β has recently been shown to play a role in the oncogenic gene regulation activities of cyclin D1 (25). E2F6, a member of the E2F family, mediates the expression of a variety of genes with products participating in the regulation of cell proliferation (26), several which (*RRM1*, *RFC4*, *BLM*, *SLBP*, *RRM2*, *PCNA*, *KCNK1*, *RFC3*, and *EED*) were down-regulated in this study.

In addition, flavopiridol reduced the expression of genes with products participating in basal transcription

such as *TAF7*, *TAF5*, and *TFIIH* (21). Whether the decrease in transcription factor expression is the result of a direct action of flavopiridol, is mediated through an effect on a signaling pathway(s) such as those involving *DKK1* or members of the *MAPK* family (Table 1), or involves some other process requires further investigation. In addition to altering the expression of specific transcription factors, flavopiridol reduced the expression of 22 genes involved in regulation of the cell cycle. Of potential significance are the cell cycle–related gene products for aurora kinase B, *BUB1*, cyclin B2, and cdk 7. Aurora kinase B, *BUB1*, and cyclin B2 participate in mitotic arrest; *BUB1* is also part of the mitotic spindle checkpoint (27). Decreased levels of these proteins may allow cells to proceed through mitosis in the presence of flavopiridol-induced injury and/or metabolic disruptions, which may further contribute to the cytotoxic process. In addition to cell cycle regulation, cdk 7 forms the cdk-activating kinase in combination with cyclin H and methionine adenosyltransferase. Cdk-activating kinase in turn forms a component of *TFIIH* and helps regulate RNA polymerase II. Therefore, a reduction in cdk 7 provides an additional pathway contributing to a decrease in transcription. Thus, although far from establishing causal relationships, these microarray data suggest that a general feature of flavopiridol-induced cell death may involve compromised transcriptional regulation and an altered mitotic checkpoint.

Although the majority of changes involved decreased expression, there were a significant number of genes (21) with increased expression in each of the solid tumor cell lines after flavopiridol exposure. With respect to functional categories, most of the up-regulated genes were either involved in intercellular signaling including Annexin 5, *CD99*, HLA-C, and β2-microglobulin or in cellular structure such as proteoglycan 1 secretory granule, histone 2, and ribosomal proteins L41 and L12. This is also consistent with the results of Daoud et al. (21) who noted an up-regulation of similar proteins involved in intercellular signaling after treatment of cells with the chemotherapeutic agent topotecan. In a lymphoma cell line treated with 1 μmol/L flavopiridol, Lam et al. (28) reported that c-*myc* mRNA levels were reduced, which they attributed to an inhibition of P-TEFb activity. However, in each of the solid tumor cell lines evaluated in the current report, c-*myc* expression was increased after flavopiridol treatment. Whether this reflects a cell type–dependent effect or is due to the different flavopiridol concentrations used in the two studies remains to be determined. Although the significance in cellular response to flavopiridol is not readily apparent, the elevated expression of certain genes suggests that flavopiridol-induced cell death does not involve a nonspecific, general inhibition of transcription.

In addition to potential mechanistic implications, such a flavopiridol death transcriptome may have applications to investigations of tumor pharmacodynamics. Currently, drug plasma levels are used to provide an indication of the potential for tumor control based on effective concentrations defined in preclinical studies. However, this clearly does not take into account sensitivity of an individual tumor or the actual drug levels reaching the tumor. In the studies described here, the flavopiridol transcriptional signature determined after 24 hours of flavopiridol exposure corresponded to 90% cell death, which was as determined 12 to 14 days later using a colony-forming assay. If a flavopiridol death transcriptome can be defined for *in vivo* tumors, then microarray analysis of gene expression performed on biopsy specimens obtained after drug treatment may provide insight into the ultimate response of an individual tumor. Moreover, such a transcriptome may be used to determine whether an agent actually reaches a tumor growing in a physiologic sanctuary such as in the central nervous system. Whereas we have focused on flavopiridol, the identification of a transcriptome corresponding to cell death may also be applicable to other forms of cancer treatment with respect to pharmacodynamics. Clearly, this is speculation and will require extensive studies initially using xenograft models.



**References**


**1.** Sedlacek H, Czech J, Naik R, et al. Flavopiridol (L86-8275; NSC 649890), a new kinase inhibitor for tumor therapy. Int J Oncol 1996;9:1143-68.

**2.** Senderowicz A, Headlee D, Stinson S, Lush RNK, Villaalba L, Hill K, et al. Phase I trial of continuous infusion flavopiridol, a novel cyclin-dependent kinase inhibitor, in patients with refractory neoplasms. J Clin Oncol 1998;16:2986-99.

**3.** Tan A, Headlee D, Messmann R, et al. Phase I clinical and pharmacokinetic study of flavopiridol administered as a daily 1-hour infusion in patients with advanced neoplasms. J Clin Oncol 2002;20:4074-82.

**4.** Thomas J, Tutsch K, Cleary J, et al. Phase I clinical and pharmacokinetic trial of the cyclin-dependent kinase inhibitor flavopiridol. Cancer Chemother Pharmacol 2002;50:465-72.

**5.** Losiewicz M, Carlson B, Kaur G, Sausville E, Worland P. Potent inhibition of CDC2 kinase activity by the flavonoid L86-8275. Biochem Biophys Res Commun 1994;201:589-95.

**6.** Carlson B, Dubay M, Sausville E, Brizuela L, Worland P. Flavopiridol induces $G_1$ arrest with inhibition of cyclin-dependent kinase (CDK) 2 and CDK4 in human breast carcinoma lines. Cancer Res 1996;56:2973-8.

**7.** Carlson B, Lahusen T, Singh S, et al. Down-regulation of cyclin D1 by transcriptional repression in MCF-7 human breast carcinoma cells induced by flavopiridol. Cancer Res 1999;59:4634-41.

**8.** Chao S, Price D. Flavopiridol inactivates P-TEFb and blocks most RNA polymerase II transcription *in vivo.* J Biol Chem 2001;276:31793-9.

**9.** Wittmann S, Bali P, Donapaty S, Nimmanapalli R, Guo F, Yamaguchi H, et al. Flavopiridol down-regulates antiapoptotic proteins and sensitizes human breast cancer cells to epothilone B-induced apoptosis. Cancer Res 2003;63:93-9.

**10.** Bible K, Bible R, Kottke T, et al. Favopiridol binds to duplex DNA. Cancer Res 2000;60:2419-28.

**11.** Simon R, Radmacher M, Dobbin K. Design of studies using DNA microarrays. Genet Epidemiol 2002;23:21-36.

**12.** Bertucci F, Viens P, Tagett R, Nguyen C, Houlgatte R, Birnbaum D. DNA arrays in clinical oncology: promises and challenges. Lab Invest 2003;83:305-16.

**13.** Clarke P, Poele R, Wooster R, Workman P. Gene expression microarray analysis in cancer biology, pharmacology, and drug development: progress and potential. Biochem Pharmacol 2003;62:1311-36.

**14.** Clarke P, George M, Easdale S, Cunningham D, Swift I, Hill M, et al. Molecular pharmacology of cancer therapy in human colorectal cancer by gene expression profiling. Cancer Res 2003;63:6855-63.

**15.** Taxman D, MacKeigan J, Clements C, Bergstralh D, Ting J.

Transcription profiling of targets for combination therapy of lung carcinoma with paclitaxel and mitogen-activated protein/extracellular signal-regulated kinase kinase inhibitor. Cancer Res 2003;63:5095-104.

**16.** Cheok M, Yang W, Pui C, et al. Treatment-specific changes in gene expression discriminate *in vivo* drug response in human leukemia cells. Nat Genet 2003;34:85-90.

**17.** Chuang Y, Chen Y, Gadisetti V, et al. Gene expression after treatment with hydrogen peroxide, menadione, or *t*-butyl hydroperoxide in breast cancer cells. Cancer Res 2002;62:6246-54.

**18.** Ross D, Scherf U, Eisen M, et al. Systematic variation in gene expression patterns in human cancer cell lines. Nat Genet 2000;24:227-35.

**19.** Druker B. Perspectives on the development of a molecularly targeted agent. Cancer Cell 2002;1:31-6.

**20.** Senderowicz A, Sausville E. Preclinical and clinical development of cyclin-dependent kinase modulators. J Natl Cancer Inst 2000;92:376-87.

**21.** Daoud S, Munson P, Reinhold W, et al. Impact of p53 knockout and topotecan treatment on gene expression profiles in human colon carcinoma cells: a pharmacogenomic study. Cancer Res 2003;63: 2782-93.

**22.** Micheau O, Solary E, Hammann A, Dimanche-Boitrel M. Fas ligand-independent, FADD-mediated activation of the Fas death pathway by anticancer drugs. J Biol Chem 1999;274:7987-92.

**23.** Trauzold A, Schmiedel S, Roder C, et al. Multiple and synergistic deregulations of apoptosis-controlling genes in pancreatic carcinoma cells. Br J Cancer 2003;89:1714-21.

**24.** McKnight S, Lane M, Gluecksohn-Waelsch S. Is CCAAT/enhancer-binding protein a central regulator of energy metabolism? Genes Dev 1989;3:2021-4.

**25.** Lamb J, Ramaswamy S, Ford H, et al. A mechanism of cyclin D1 action encoded in the patterns of gene expression in human cancer. Cell 2003;114:323-34.

**26.** Vernell R, Helin K, Muller H. Identification of target genes in the p16ink4a-pRB-E2F pathway. J Biol Chem 2003;278:46124-37.

**27.** Jallepalli P, Lengauer C. Chromosome segregation and cancer: cutting through the mystery. Nat Rev Cancer 2001;1:109-17.

**28.** Lam L, Pickeral O, Peng A, et al. Genomic-scale measurement of mRNA turnover and the mechanisms of action of the anti-cancer drug flavopiridol. Genome Biol 2001;2:1-11.